Axial and Torsional Load-Type Sequencing in Cumulative Fatigue: Low Amplitude Followed by High Amplitude Loading

P. J. Bonacuse[1] and S. Kalluri[2]

[1] US Army Research Laboratory, NASA Glenn Research Center, Cleveland, OH, USA

[2] Ohio Aerospace Institute, NASA Glenn Research Center, Cleveland, OH, USA

ABSTRACT: *The experiments described herein were performed to determine whether damage imposed by axial loading interacts with damage imposed by torsional loading. This paper is a follow on to a study [1] that investigated effects of load-type sequencing on the cumulative fatigue behavior of a cobalt base superalloy, Haynes 188 at 538°C. Both the current and the previous study were used to test the applicability of cumulative fatigue damage models to conditions where damage is imposed by different loading modes. In the previous study, axial and torsional two load level cumulative fatigue experiments were conducted, in varied combinations, with the low-cycle fatigue (high amplitude loading) applied first. In present study, the high-cycle fatigue (low amplitude loading) is applied initially. As in the previous study, four sequences (axial/axial, torsion/torsion, axial/torsion, and torsion/axial) of two load level cumulative fatigue experiments were performed. The amount of fatigue damage contributed by each of the imposed loads was estimated by both the Palmgren-Miner linear damage rule (LDR) and the non-linear damage curve approach (DCA). Life predictions for the various cumulative loading combinations are compared with experimental results.*

INTRODUCTION

Many multiaxial fatigue damage models are based on the premise that damage is a tensor, i.e., it has both magnitude and direction. If this were true, damage imposed by loading in one plane should not readily interact with subsequent damage imposed by loading in another direction. By subjecting thin-walled tubular specimens to fatigue in different loading directions, in sequence, this hypothesis can be tested.

The cyclic hardening behavior of superalloys is, at least to some extent, isotropic in nature. This hardening should influence damage accumulation even when loading is imposed in another direction.

MATERIAL, SPECIMENS, AND TEST PARAMETERS

Specimens used in this study were fabricated from hot rolled, solution annealed, Haynes 188 superalloy, bar stock. This is the same heat of material used to perform the experiments described in Ref. [1].

All experiments were performed on thin walled tubes with a gage section of nominally 26 mm outer diameter and 22 mm inner diameter. Interior surfaces were honed in an attempt to preclude crack initiation on the inner surface of the specimen. Outer surfaces were polished with final polish parallel to the specimen axis. Further details on the specimen geometry and machining specifications can be found in [2]. The baseline axial and torsional fatigue lives for this material, specimen geometry, and test temperature can be found in [1].

The specimens were heated to 538°C with an induction heating system. All specimens were subjected to sequential constant amplitude fatigue loading under strain control. The other axis was maintained in load control at zero load. The failure criterion programmed into the testing software was a 10% load drop. Five experiments were terminated due to a controller interlock. Details on the test machine, heating system and test control software can be found in [1,2].

TEST MATRIX

The test matrix for this study is shown in Table I. Seventeen different combinations of two block loading experiments were performed. The sequences were axial-axial, torsion-torsion, axial-torsion, and torsion-axial, with at least four first load level life fractions imposed in each combination. A fifth life fraction was imposed in the torsion-torsion subset. One torsional experiment was repeated as a cursory check on the expected specimen-to-specimen variability. This added up to a total of 18 tests performed for this study. Table I also contains the stabilized (half life) stresses for each load level, the number of cycles imposed, and the final crack orientation.

TABLE I: TEST MATRIX AND INTERACTION FATIGUE DATA FOR HAYNES 188 AT 538°C.

Specimen	First Load Level; ν = 0.5 Hz							Second Load Level; ν = 0.1 Hz							Crack * Orientation
	$\Delta\varepsilon_1$	$\Delta\sigma_1$ (MPa)	σ_{m1} (MPa)	$\Delta\gamma_1$	$\Delta\tau_1$ (MPa)	τ_{m1} (MPa)	n_1 (Cycles)	$\Delta\varepsilon_2$	$\Delta\sigma_2$ (MPa)	σ_{m2} (MPa)	$\Delta\gamma_2$	$\Delta\tau_2$ (MPa)	τ_{m2} (MPa)	n_2 (Cycles)	
A-A															
HYII-103	0.0067	811	-9	...	...	...	3926	0.0203	1254	-14	...	...	...	789	75°
HYII-116	0.0066	849	-6	...	...	...	7851	0.0202	1247	-14	...	...	...	758	80°
HYII-119	0.0066	882	-10	...	...	...	15702	0.0203	1244	-11	...	...	...	659	85°
HYII-114	0.0066	905	-9	...	...	...	23553	0.0205	1267	-12	...	...	...	815	90°
T-T															
HYII-117	...	...	...	0.0120	515	-1	5857	...	...	...	0.0345	731	1	1250	0°
HYII-112	...	...	...	0.0120	536	0	11714	...	...	...	0.0349	740	1	1100	0°
HYII-115	...	...	...	0.0119	554	1	23427	...	...	...	0.0346	731	0	816	0°
HYII-109	...	...	...	0.0121	521	0	23427	...	...	...	0.0347	709	2	1343	0°
HYII-118	...	...	...	0.0119	588	0	35141	...	...	...	0.0347	748	0	1467	0°
HYII-104	...	...	...	0.0120	579	-2	40998	...	...	...	0.0349	732	-2	1294	0°
A-T															
HYII-110	0.0069	841	-10	...	...	...	3926	...	...	...	0.0348	781	2	1189	0°
HYII-111	0.0069	862	-8	...	...	...	7851	...	...	...	0.0347	761	0	1218	5°
HYII-108	0.0065	892	-8	...	...	...	15702	...	...	...	0.0344	794	1	930	0°
HYII-105	0.0066	888	-9	...	...	...	23553	...	...	...	0.0346	783	2	1253	0°
T-A															
HYII-120	...	...	...	0.0121	498	0	5857	0.0201	1400	-15	...	...	...	560	90°
HYII-107	...	...	...	0.0120	523	-1	11714	0.0203	1414	-16	...	...	...	494	90°
HYII-106	...	...	...	0.0119	540	0	23427	0.0200	1432	-20	...	...	...	459	75°
HYII-113	...	...	...	0.0119	581	-1	35141	0.0204	1452	-18	...	...	...	427	80°

* Angle measured with respect to specimen axis.

RESULTS AND DISCUSSION

The initially imposed lower amplitude cyclic loading caused this solution-annealed material to isotropically harden. The magnitude of the hardening in the first load level was proportional to the number of imposed cycles. Stress range vs. cycle plots (Fig. 1) for the second load level show some interesting behavior. The lower initial life fraction experiments continue to harden during the second load level (with exception of the axial-axial where all hardened to failure). The higher initial life fraction experiments tended to cyclically soften. The material in each type of load level combination tended to converge to a similar stress range as the tests progressed.

Experiments ending with torsional loading always failed on the maximum shear strain plane in line with the specimen axis. There are some indications that these cracks may have initiated along final polishing marks. Experiments completed under axial loading all failed at or near the plane of maximum tensile stress. In the tests completed with axial loading, the 10% load drop failure criteria corresponded to an average crack length, of 20.5 mm. Somewhat longer surface cracks (27.4 mm average length) occurred in the tests completed with torsional loading.

Five of the eighteen tests stopped due to controller interlocks. Most the controller interlocks occurred due to a crack opening up on side of specimen opposite to the extensometer and/or outside the extensometer gage section. Larger final cracks and significant specimen distortion were associated with these events. Fatigue surface crack lengths were of the same order as those observed in those ended at a 10% load drop.

The results of the cumulative fatigue experiments performed for this study were compared with predictions of two load interaction models: the linear damage rule (LDR) (Eq 1), often referred to as Miner's rule, and the damage curve approach (DCA) (Eq 2)[3].

$$\left(\frac{n_2}{N_2}\right) = 1 - \left(\frac{n_1}{N_1}\right) \tag{1}$$

$$\left(\frac{n_2}{N_2}\right) = 1 - \left(\frac{n_1}{N_1}\right)^{\left(\frac{N_1}{N_2}\right)^{0.4}} \tag{2}$$

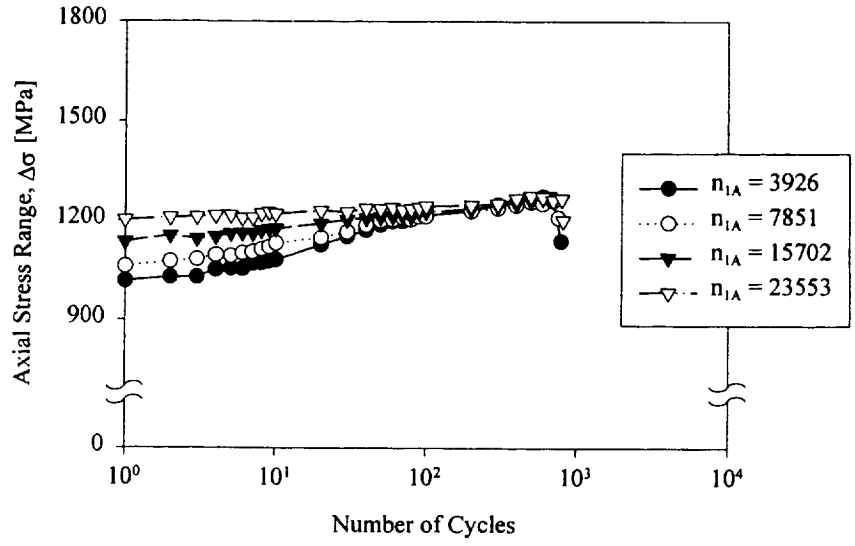

(a) Axial-Axial

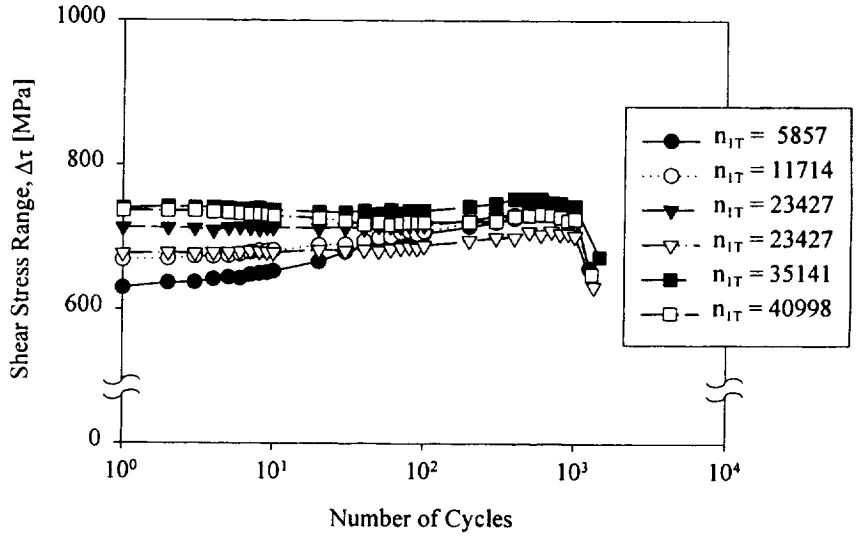

(b) Torsion-Torsion

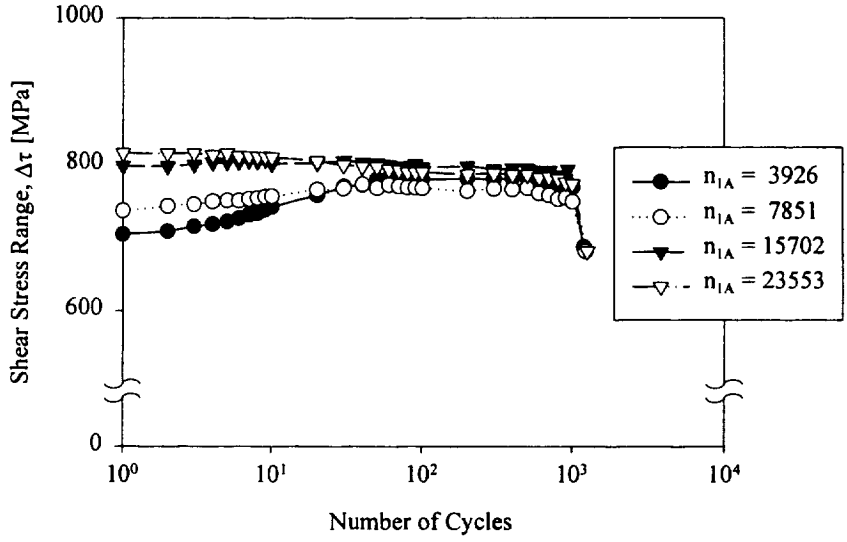

(c) Axial-Torsion

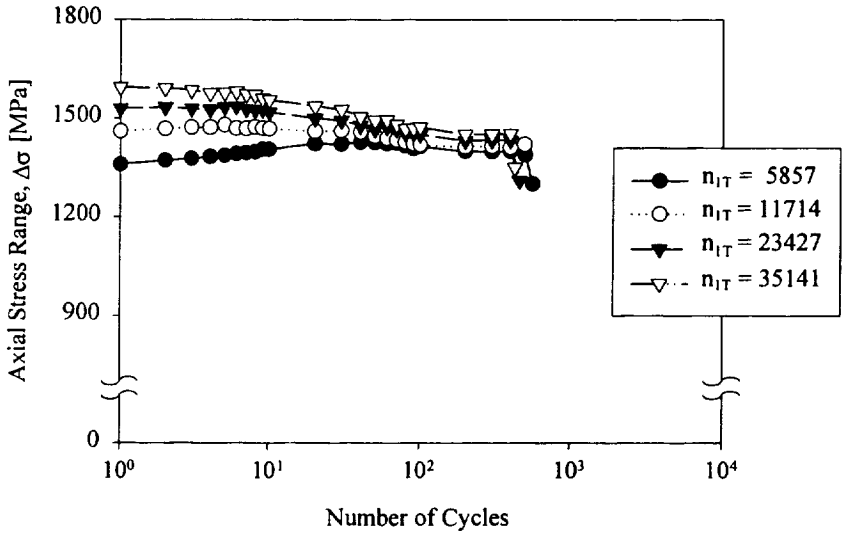

(d) Torsion-Axial

Figure 1: Cyclic hardening behavior of low strain amplitude followed by high strain amplitude tests

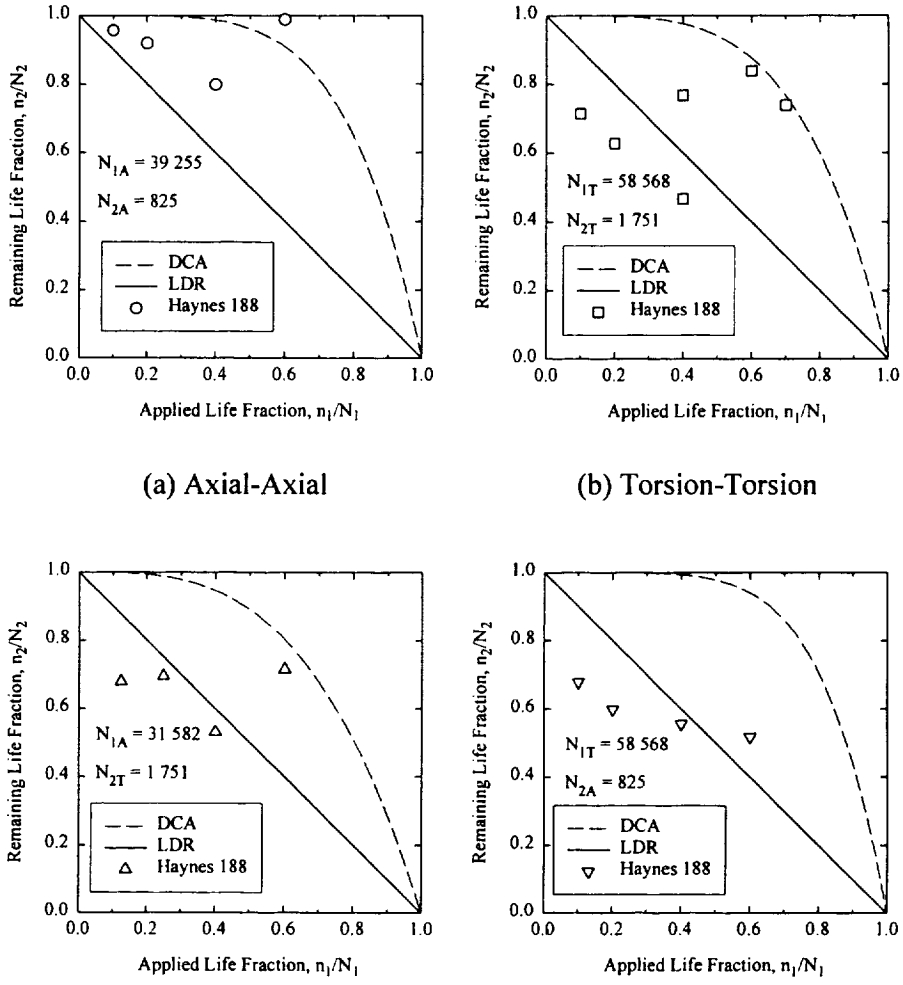

Figure 2: Fatigue life estimation of low amplitude followed by high amplitude fatigue experiments.

The results of the axial-axial, torsion-torsion, axial-torsion, and torsion-axial experiments are shown in Fig. 2. It's clear that neither cumulative damage model predicts the observed behavior adequately. In most cases, the LDR seems to more closely approximate the observed behavior for

lower initially applied life fractions ($n_1/N_1 \leq 0.4$) whereas the DCA model seems to do better with the higher ($n_1/N_1 > 0.4$) initially applied life fractions.

The extent of isotropic hardening in the material seems to effect the subsequent deformation and damage accumulation. As shown in Fig. 3, the magnitude of the equivalent plastic strain in the first load level is inversely correlated with the sum of the life fractions.

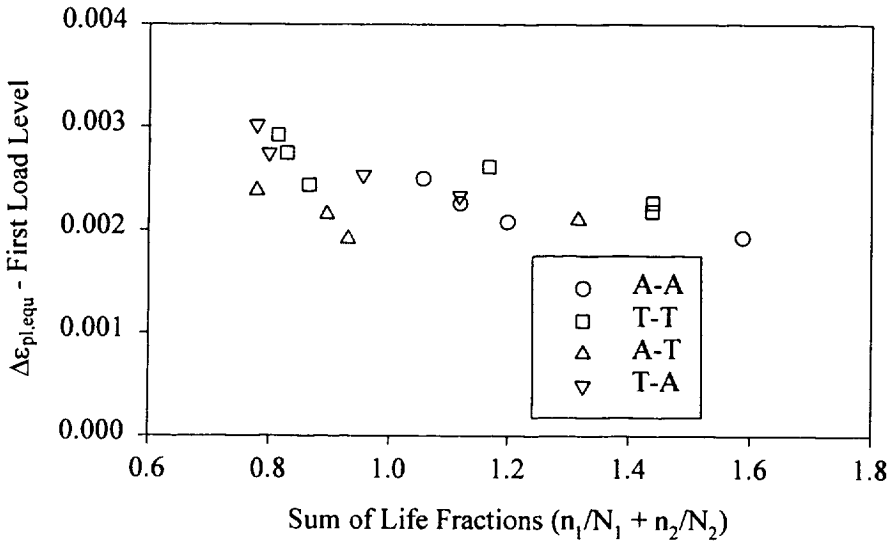

Figure 3: Equivalent plastic strain in first load level vs. sum of life fractions

CONCLUSIONS

1) Neither the LDA nor the DCA predicted the interactions in these experiments particularly well. Predictions by the LDA were marginally better than those by the DCA.

2) The fatigue life data suggest some transition behavior that may be linked to the extent of work hardening imposed by the initial load level; the greater the life fraction expended in lower amplitude loading, the greater the chance of having a sum of life fractions more than unity.

REFERENCES

1. Kalluri, S. and Bonacuse, P. J. (2000), In: *STP 1387 -- Multiaxial Fatigue and Deformation: Testing and Prediction*, pp. 281-301, S. Kalluri and P. J. Bonacuse (Eds)., ASTM, West Conshohocken, PA
2. Bonacuse, P. J., and Kalluri, S. (1993) *JTEVA* **21**, 160.
3. Manson, S. S. and Halford, G. R. (1981) *Int. J. Fracture* **17**, 169.